École et observatoire des sciences de la Terre
Université de Strasbourg
Laboratoire d'Hydrologie et de Géochimie de Strasbourg
DESTRESS
Demonstration of soft stimulation treatments of geothermal reservoirs
European Commission
THE FRAMEWORK PROGRAMME FOR RESEARCH AND INNOVATION HORIZON 2020

The potential for acid stimulation of a deep geothermal reservoir: an experimental investigation

Jamie I. FARQUHARSON[1]; Patrick BAUD[1]; Bastien WILD[2]; Alexandra R. L. KUSHNIR[1]

[1]Institut de Physique de Globe de Strasbourg
[2]Laboratoire d'Hydrologie et de Géochimie de Strasbourg
Ecole et Observatoire des Sciences de la Terre
5 rue René Descartes
1 rue Blessig
67084 Strasbourg cedex, France

REFERENCE:
Farquharson, J. I., Kushnir, A. R., Wild, B., & Baud, P. (2020). Physical property evolution of granite during experimental chemical stimulation. Geothermal Energy, 8, 1-24.

Introduction

The geothermal power plant at Soultz-sous-Forêts in France has been proposed as a target for potential enhancement through **acid stimulation**. In order to determine the feasibility and impact of acid stimulation of the deep reservoir rocks, an experimental campaign has been undertaken under the auspices of the DESTRESS Horizon-2020 project. Experiments have been designed to constrain the evolution of physical (**mass**, **porosity**, **permeability**) and mechanical (**compressive strength**) properties of the reservoir material as a function of different acid treatments.

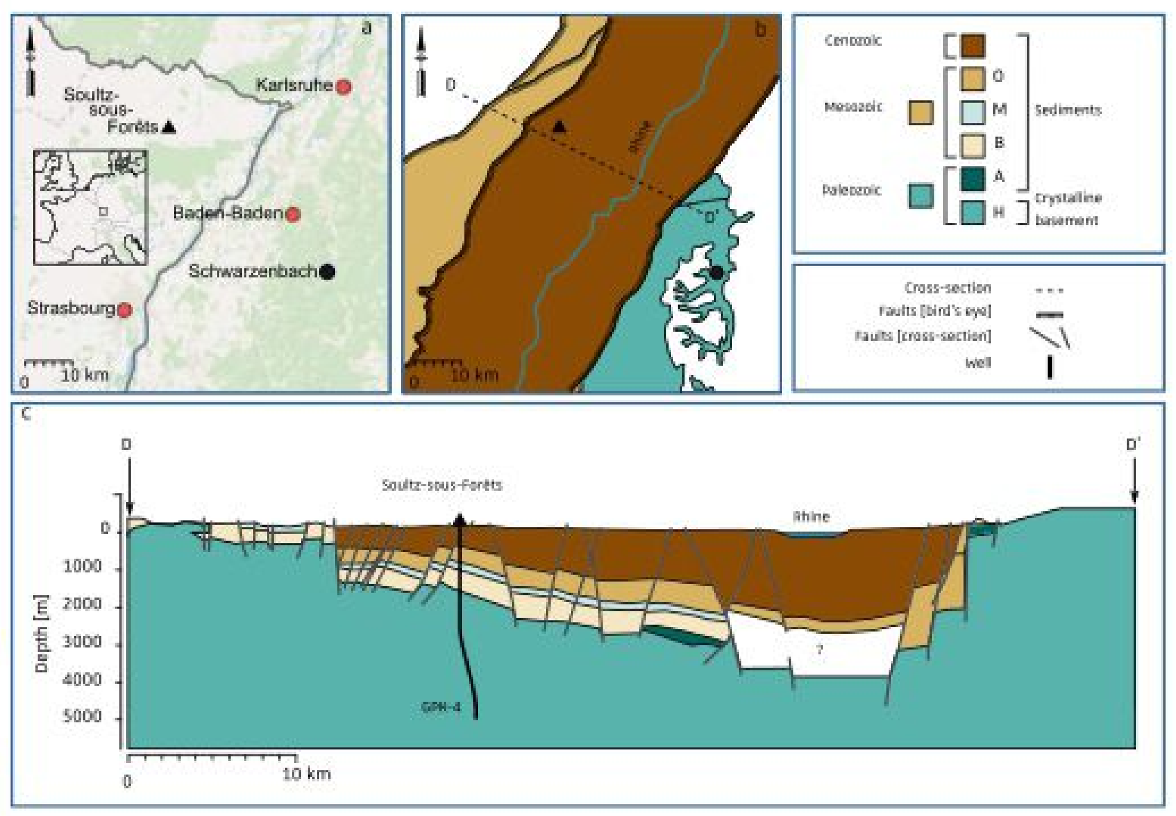

Figure 1: Site location and sampling area.
[a] Location map of Soultz-sous-Forêts and Schwarzenbach.
[b] Geological map of the area shown in [a], indicating location of cross-section in [c].
[c] Geological cross-section of the Upper Rhine Graben region. The open-hole section of the GPK-4 well is situated in the Hercynian crystalline basement.

The starting material for these experiments were collected from a site near the Schwarzenbach Dam in Germany, where the granitic basement underlying the Soultz-sous-Forêts plant is outcropping and accessible (**Figure 1**). This material is a good analogue for the granite at around 5000 m depth, where the open-hole section of the GPK-4 well is situated.

The granites have been categorised into three separate groups (**Figure 2**):
G2M-A: a fine-grained leucocratic granite containing **muscovite** and **biotite**;
G2M-B: a slightly hydrothermally altered granite containing muscovite, biotite, and additional **secondary minerals**;
G2M-F: an unaltered granite identical to G2M-A, but containing abundant **fractures**.

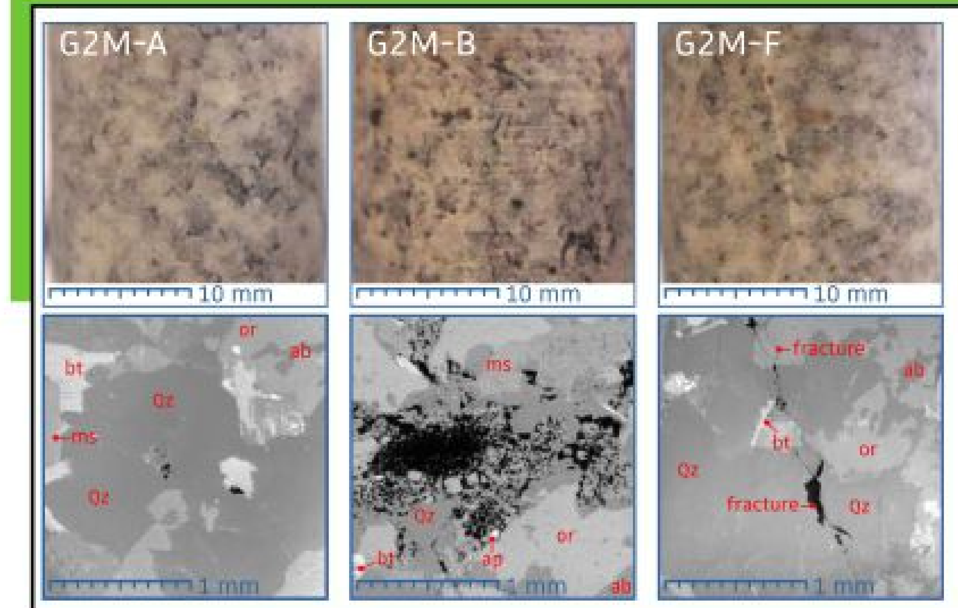

Figure 2: Examples of three classes of granite collected at Schwarzenbach.
[above] sample photographs.
[below] Scanning Electron Microscope images.
Mineral phases identified using X-ray fluorescence and energy dispersive X-ray microanalysis:
Qz = quartz;
or = orthoclase;
ab = albite;
bt = biotite;
ms = muscovite;
ap = apatite

Methods

Suites of samples (20 x 40 mm) were immersed in acid solutions for varying periods of time. For the purposes of this study, two different concentrations of hydrochloric acid were prepared (0.2 and 2.0 N HCl), by combining concentrated HCl with distilled and deionised water. Mass, porosity, and permeability of all samples were measured prior to immersion. Periodically, samples were removed and recharacterised in order to monitor the evolution of these physical properties. Additionally, some samples underwent thermal stressing in a furnace whereby they were heated at 1 °C min^{-1} until a target temperature *T*, left to dwell at that temperature for 120 min, then cooled again at the same rate. A control suite of granites was also set aside for mechanical testing (uniaxial compressive strength) against which to compare acid-treated samples. Hereafter, we show the relative change in physical (or mechanical) properties, such that for any property a, the relative change $a' = a/a^*$, where a^* is the post-treatment value.

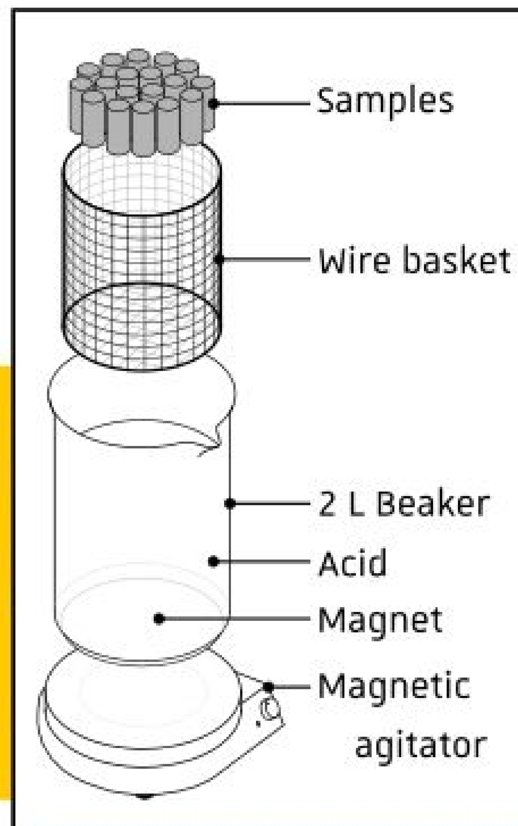

↑Figure 3: Schematic of simple batch reactor. Samples are at ambient pressure and temperature.

Results and Discussion

Naturally fractured samples (G2M-F) are markedy more permeable (10^{-16} m^2). Further, the altered granite (G2M-B) is more permeable than the unaltered (G2M-A), with permeabilities on the order of 10^{-18} and $<10^{-21}$ m^2, respectively.

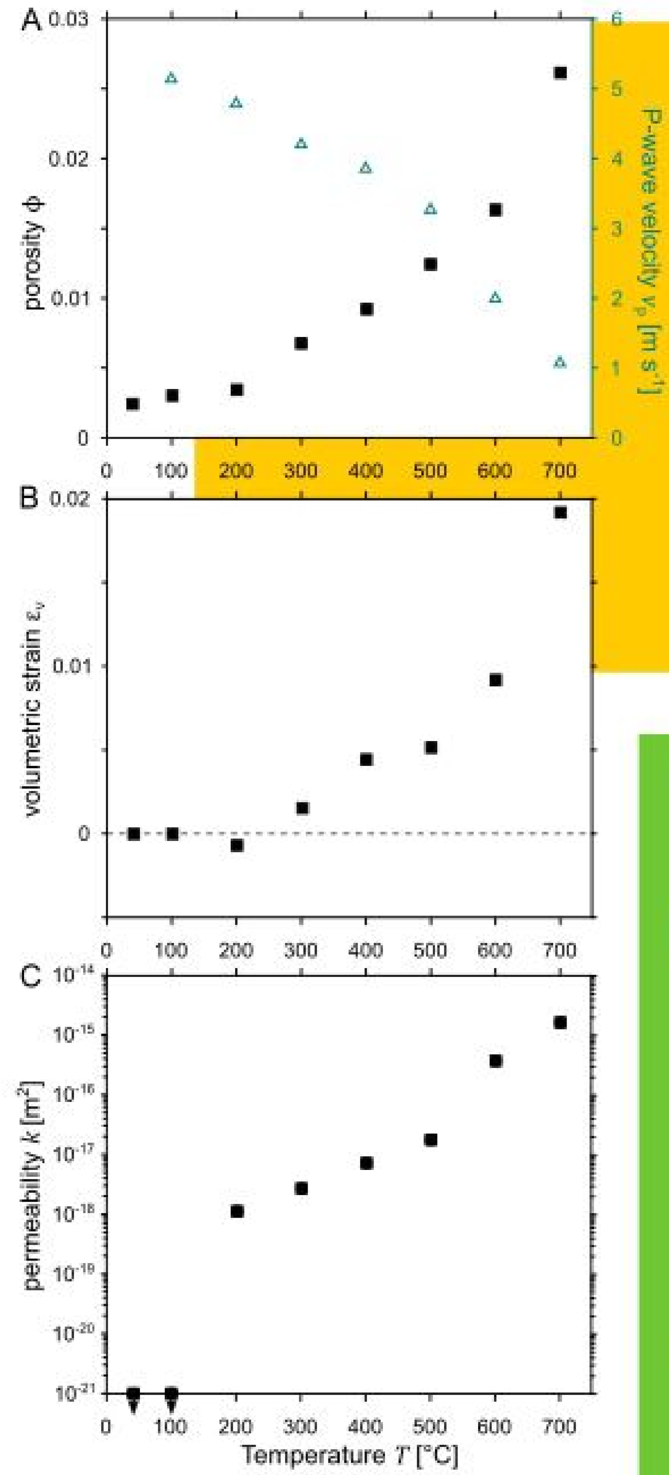

↑Figure 4: Evolution of physical properties of an unaltered granite (G2M-A) after incremental thermal stress treatment

The initial permeability of G2M-A is extremely low; however, by incrementally heating to higher temperatures (**Figure 4A-C**), we observe an onset of measurable permeability between 200 and 300 °C, coinciding with an uptick in porosity formation (from <0.3vol.% to 2.6vol.%), presumably due to thermal microcracking (a product of thermal expansion mismatch between constituent grains). By thermally stressing samples to 600 °C and higher, permeability was increased by over 5 orders of magnitude (up to 10^{-16} m^2).

Immersion in 0.2 N HCl increased permeability of intact G2M-A samples from $<10^{-21}$ to $>10^{-18}$ m^2. Under the same conditions, G2M-B samples increased in permeability by a factor of ~1.5. Permeability of G2M-B samples was only increased by a factor of 2 by increasing the acid concentration by an order of magnitude (2.0 N HCl). Data are shown in **Figure 5A-C**, which gives the mass loss, porosity change and permeability change (relative to the initial values) as a function of immersion time.

When pre -fractured samples (both naturally and thermally fractured) were immersed in 0.2 N HCl for 1008 hours, a slight **decrease in permeability** was observed. This is presumably due to their high pre-stimulation permeabilities and the remobilisation rather than removal of any dissolvable minerals.

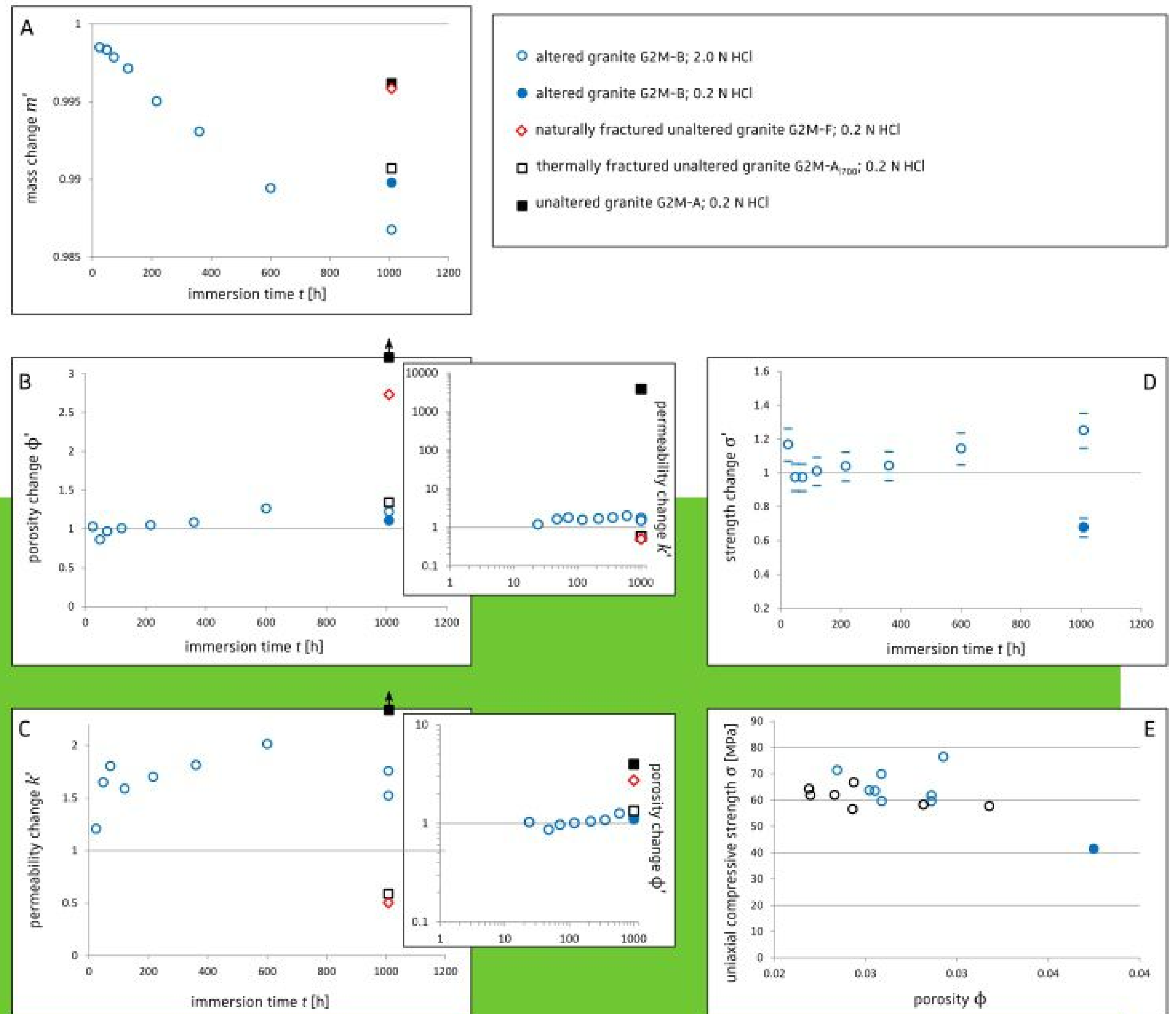

↑Figure 5: Evolution of physical and mechanical properties as a function of acid immersion. [A] Mass evolution with immersion time [B] Porosity evolution [C[Permeability evolution [D] Strength evolution [E] Uniaxial compressive strength against porosity for acid treated (blue symbols) and untreated (black symbols) samples.

Strength evolution is shown in Figure 5D and 5E. Notably, when a stronger acid solution was used, strength appears to increase relative to the control suite. With 0.2 N concentration, strength is decreased somewhat, likely due to the dissolution-induced increase in porosity . Future work will explore the apparent relationship between strength evolution and acid concentration. Moreover, ongoing fluid and chemical analyses will shed light on the rate and magnitude of dissolution and precipitation mechanisms at play.